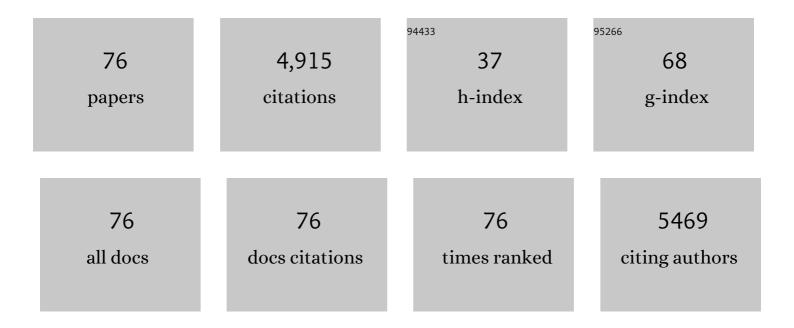


List of Publications by Year in descending order

Source: https://exaly.com/author-pdf/2772527/publications.pdf Version: 2024-02-01



\\/FLLL

#	Article	IF	CITATIONS
1	Mechanisms of fluoride uptake by surface-modified calcite: A 19F solid-state NMR and TEM study. Chemosphere, 2022, 294, 133729.	8.2	7
2	Long-Range and Short-Range Structures of Multimetallic Layered Double Hydroxides. Journal of Physical Chemistry C, 2022, 126, 5311-5322.	3.1	10
3	Zn stable isotope fractionation during adsorption onto todorokite: A molecular perspective from X-ray absorption spectroscopy and density functional theory. Geochimica Et Cosmochimica Acta, 2022, 327, 116-136.	3.9	12
4	Molecular scale assessment of defluoridation of coal-mining wastewater by calcined Mg/Al layered double hydroxide using 19F solid-state NMR, XPS, and HRTEM. Chemosphere, 2022, 303, 135072.	8.2	12
5	A review of cadmium sorption mechanisms on soil mineral surfaces revealed from synchrotron-based X-ray absorption fine structure spectroscopy: Implications for soil remediation. Pedosphere, 2021, 31, 11-27.	4.0	41
6	Combining zinc desorption with EXAFS speciation analysis to understand Zn mobility in mining and smelting affected soils in Minas Gerais, Brazil. Science of the Total Environment, 2021, 754, 142450.	8.0	11
7	Linking Environmental Science with Geochemistry. Bulletin of Environmental Contamination and Toxicology, 2021, 106, 1-1.	2.7	2
8	Speciation transformation of Pb during palygorskite sorption-calcination process: Implications for Pb sequestration. Applied Geochemistry, 2021, 124, 104850.	3.0	7
9	Cadmium Isotope Fractionation during Adsorption and Substitution with Iron (Oxyhydr)oxides. Environmental Science & Technology, 2021, 55, 11601-11611.	10.0	58
10	Phosphate uptake by calcite: Constraints of concentration and pH on the formation of calcium phosphate precipitates. Chemical Geology, 2021, 579, 120365.	3.3	10
11	EXAFS investigation of Ni(â;) sorption at the palygorskite-solution interface: New insights into surface-induced precipitation phenomena. Geochimica Et Cosmochimica Acta, 2021, 314, 85-107.	3.9	14
12	Enhanced Fluoride Uptake by Layered Double Hydroxides under Alkaline Conditions: Solid-State NMR Evidence of the Role of Surface >MgOH Sites. Environmental Science & Technology, 2021, 55, 15082-15089.	10.0	22
13	Use of lanthanum/aluminum co-modified granulated attapulgite clay as a novel phosphorus (P) sorbent to immobilize P and stabilize surface sediment in shallow eutrophic lakes. Chemical Engineering Journal, 2020, 385, 123395.	12.7	81
14	Enrichment and source identification of Cd and other heavy metals in soils with high geochemical background in the karst region, Southwestern China. Chemosphere, 2020, 245, 125620.	8.2	124
15	Evaluation of various approaches to predict cadmium bioavailability to rice grown in soils with high geochemical background in the karst region, Southwestern China. Environmental Pollution, 2020, 258, 113645.	7.5	126
16	Preparation of the Lanthanum–Aluminum-Amended Attapulgite Composite as a Novel Inactivation Material to Immobilize Phosphorus in Lake Sediment. Environmental Science & Technology, 2020, 54, 11602-11610.	10.0	45
17	Improvement of quantitative solution 31P NMR analysis of soil organic P: a study of spin–lattice relaxation responding to paramagnetic ions. Geochemical Transactions, 2020, 21, 3.	0.7	2
18	Speciation Transformation of Phosphorus in Poultry Litter during Pyrolysis: Insights from X-ray Diffraction, Fourier Transform Infrared, and Solid-State NMR Spectroscopy. Environmental Science & Technology, 2019, 53, 13841-13849.	10.0	43

#	Article	IF	CITATIONS
19	Molecular-scale investigation of fluoride sorption mechanism by nanosized hydroxyapatite using 19F solid-state NMR spectroscopy. Journal of Colloid and Interface Science, 2019, 557, 357-366.	9.4	30
20	Molecular speciation of phosphorus in phosphogypsum waste by solid-state nuclear magnetic resonance spectroscopy. Science of the Total Environment, 2019, 696, 133958.	8.0	17
21	Fluoride uptake by three lanthanum based nanomaterials: Behavior and mechanism dependent upon lanthanum species. Science of the Total Environment, 2019, 683, 609-616.	8.0	45
22	Environmental applications of metal stable isotopes: Silver, mercury and zinc. Environmental Pollution, 2019, 252, 1344-1356.	7.5	36
23	Formation of Cd precipitates on \hat{I}^3 -Al2O3: Implications for Cd sequestration in the environment. Environment International, 2019, 126, 234-241.	10.0	31
24	Effect of Î ³ -manganite particle size on Zn2+ coordination environment during adsorption and desorption. Applied Clay Science, 2019, 168, 68-76.	5.2	9
25	Identification of Fe and Zr oxide phases in an iron-zirconium binary oxide and arsenate complexes adsorbed onto their surfaces. Journal of Hazardous Materials, 2018, 353, 340-347.	12.4	26
26	Characterization of Lead Uptake by Nano-Sized Hydroxyapatite: A Molecular Scale Perspective. ACS Earth and Space Chemistry, 2018, 2, 599-607.	2.7	33
27	Iron and Arsenic Speciation During As(III) Oxidation by Manganese Oxides in the Presence of Fe(II): Molecular-Level Characterization Using XAFS, Mössbauer, and TEM Analysis. ACS Earth and Space Chemistry, 2018, 2, 256-268.	2.7	32
28	The Important Role of Layered Double Hydroxides in Soil Chemical Processes and Remediation: What We Have Learned Over the Past 20 Years. Advances in Agronomy, 2018, 147, 1-59.	5.2	29
29	Competitive sorption of Ni and Zn at the aluminum oxide/water interface: an XAFS study. Geochemical Transactions, 2018, 19, 9.	0.7	20
30	Remediation techniques for heavy metal-contaminated soils: Principles and applicability. Science of the Total Environment, 2018, 633, 206-219.	8.0	1,064
31	A novel multi-reaction model for kinetics of Zn release from soils: Roles of soil binding sites. Journal of Colloid and Interface Science, 2018, 514, 146-155.	9.4	22
32	Contrasting effects of inorganic and organic fertilisation regimes on shifts in Fe redox bacterial communities in red soils. Soil Biology and Biochemistry, 2018, 117, 56-67.	8.8	48
33	Peroxymonosulfate activation by iron(III)-tetraamidomacrocyclic ligand for degradation of organic pollutants via high-valent iron-oxo complex. Water Research, 2018, 147, 233-241.	11.3	161
34	Sources and Pathways of Formation of Recalcitrant and Residual Phosphorus in an Agricultural Soil. Soil Systems, 2018, 2, 45.	2.6	20
35	Transformation of Phosphorus in Speciation and Bioavailability During Converting Poultry Litter to Biochar. Frontiers in Sustainable Food Systems, 2018, 2, .	3.9	21
36	Zinc Isotope Fractionation during Sorption onto Al Oxides: Atomic Level Understanding from EXAFS. Environmental Science & Technology, 2018, 52, 9087-9096.	10.0	40

#	Article	IF	CITATIONS
37	Introducing hydrate aluminum into porous thermally-treated calcium-rich attapulgite to enhance its phosphorus sorption capacity for sediment internal loading management. Chemical Engineering Journal, 2018, 348, 704-712.	12.7	54
38	Ecological risk assessment on heavy metals in soils: Use of soil diffuse reflectance mid-infrared Fourier-transform spectroscopy. Scientific Reports, 2017, 7, 40709.	3.3	22
39	Macroscopic and microscopic investigation of adsorption and precipitation of Zn on Î ³ -alumina in the absence and presence of As. Chemosphere, 2017, 178, 309-316.	8.2	9
40	An EXAFS investigation of the mechanism of competitive sorption between Co(II) and Ni(II) at Î ³ -alumina/solution interface. Acta Geochimica, 2017, 36, 462-464.	1.7	4
41	Enhanced Dissolution and Transformation of ZnO Nanoparticles: The Role of Inositol Hexakisphosphate. Environmental Science & Technology, 2016, 50, 5651-5660.	10.0	60
42	Fe(II) sorption on pyrophyllite: Effect of structural Fe(III) (impurity) in pyrophyllite on nature of layered double hydroxide (LDH) secondary mineral formation. Chemical Geology, 2016, 439, 152-160.	3.3	28
43	Oxidation of Benzene by Persulfate in the Presence of Fe(III)- and Mn(IV)-Containing Oxides: Stoichiometric Efficiency and Transformation Products. Environmental Science & Technology, 2016, 50, 890-898.	10.0	257
44	Redox Reactions between Mn(II) and Hexagonal Birnessite Change Its Layer Symmetry. Environmental Science & Technology, 2016, 50, 1750-1758.	10.0	102
45	Effects of crystallite size on the structure and magnetism of ferrihydrite. Environmental Science: Nano, 2016, 3, 190-202.	4.3	77
46	An invisible soil acidification: Critical role of soil carbonate and its impact on heavy metal bioavailability. Scientific Reports, 2015, 5, 12735.	3.3	66
47	Characterizing Phosphorus Speciation of Chesapeake Bay Sediments Using Chemical Extraction, ³¹ P NMR, and X-ray Absorption Fine Structure Spectroscopy. Environmental Science & Technology, 2015, 49, 203-211.	10.0	69
48	The effects of iron(II) on the kinetics of arsenic oxidation and sorption on manganese oxides. Journal of Colloid and Interface Science, 2015, 457, 319-328.	9.4	40
49	Size-dependent sorption of myo-inositol hexakisphosphate and orthophosphate on nano-γ-Al2O3. Journal of Colloid and Interface Science, 2015, 451, 85-92.	9.4	33
50	The regime and P availability of omitting P fertilizer application for rice in rice/wheat rotation in the Taihu Lake Region of southern China. Journal of Soils and Sediments, 2015, 15, 844-853.	3.0	25
51	Effect of Iron(II) on Arsenic Sequestration by δ-MnO ₂ : Desorption Studies Using Stirred-Flow Experiments and X-Ray Absorption Fine-Structure Spectroscopy. Environmental Science & Technology, 2015, 49, 13360-13368.	10.0	26
52	Effect of iron oxide reductive dissolution on the transformation and immobilization of arsenic in soils: New insights from X-ray photoelectron and X-ray absorption spectroscopy. Journal of Hazardous Materials, 2014, 279, 212-219.	12.4	77
53	Mechanism of Myo-inositol Hexakisphosphate Sorption on Amorphous Aluminum Hydroxide: Spectroscopic Evidence for Rapid Surface Precipitation. Environmental Science & Technology, 2014, 48, 6735-6742.	10.0	103
54	Real-time QEXAFS spectroscopy measures rapid precipitate formation at the mineral–water interface. Nature Communications, 2014, 5, 5003.	12.8	47

#	Article	IF	CITATIONS
55	Versatile inorganic-organic hybrid WO x -ethylenediamine nanowires: Synthesis, mechanism and application in heavy metal ion adsorption and catalysis. Nano Research, 2014, 7, 903-916.	10.4	59
56	Sorption and desorption characteristics of organic phosphates of different structures on aluminium (oxyhydr)oxides. European Journal of Soil Science, 2014, 65, 308-317.	3.9	69
57	Different effects of copper (II), cadmium (II) and phosphate on the sorption of phenanthrene on the biomass of cyanobacteria. Journal of Hazardous Materials, 2013, 261, 21-28.	12.4	35
58	Solid-State NMR Spectroscopic Study of Phosphate Sorption Mechanisms on Aluminum (Hydr)oxides. Environmental Science & Technology, 2013, 47, 130725144353009.	10.0	30
59	Effect of Ferrihydrite Crystallite Size on Phosphate Adsorption Reactivity. Environmental Science & Technology, 2013, 47, 10322-10331.	10.0	191
60	Inhibition Mechanisms of Zn Precipitation on Aluminum Oxide by Glyphosate: A ³¹ P NMR and Zn EXAFS Study. Environmental Science & Technology, 2013, 47, 4211-4219.	10.0	37
61	Molecular level investigations of phosphate sorption on corundum (α-Al2O3) by 31P solid state NMR, ATR-FTIR and quantum chemical calculation. Geochimica Et Cosmochimica Acta, 2013, 107, 252-266.	3.9	94
62	Adsorption of carbon dioxide on Al/Fe oxyhydroxide. Journal of Colloid and Interface Science, 2013, 400, 1-10.	9.4	22
63	Characteristics of Phosphate Adsorption-Desorption Onto Ferrihydrite. Soil Science, 2013, 178, 1-11.	0.9	155
64	Effect of magnesium oxide on adsorption of Cd2+ from aqueous solution. RSC Advances, 2012, 2, 5178.	3.6	12
65	Bismuth 2,6-pyridinedicarboxylates: Assembly of molecular units into coordination polymers, CO2 sorption and photoluminescence. Dalton Transactions, 2012, 41, 4126.	3.3	60
66	Formation of hydroxylapatite from co-sorption of phosphate and calcium by boehmite. Geochimica Et Cosmochimica Acta, 2012, 85, 289-301.	3.9	38
67	Formation of Crystalline Zn–Al Layered Double Hydroxide Precipitates on γ-Alumina: The Role of Mineral Dissolution. Environmental Science & Technology, 2012, 46, 11670-11677.	10.0	93
68	Differential Pair Distribution Function Study of the Structure of Arsenate Adsorbed on Nanocrystalline γ-Alumina. Environmental Science & Technology, 2011, 45, 9687-9692.	10.0	66
69	Phosphate adsorption on the iron oxyhydroxides goethite (α-FeOOH), akaganeite (β-FeOOH), and lepidocrocite (γ-FeOOH): a 31P NMR Study. Energy and Environmental Science, 2011, 4, 4298.	30.8	187
70	Phosphate uptake by TiO2: Batch studies and NMR spectroscopic evidence for multisite adsorption. Journal of Colloid and Interface Science, 2011, 364, 455-461.	9.4	61
71	Synthesis and Structural Characterization of a 3-D Lithium Based Metalâ~'Organic Framework Showing Dynamic Structural Behavior. Crystal Growth and Design, 2010, 10, 2801-2805.	3.0	55
72	Surface Speciation of Phosphate on Boehmite (γ-AlOOH) Determined from NMR Spectroscopy. Langmuir, 2010, 26, 4753-4761.	3.5	63

#	Article	IF	CITATIONS
73	Arsenate substitution in hydroxylapatite: Structural characterization of the Ca5(PxAs1-xO4)3OH solid solution. American Mineralogist, 2009, 94, 666-675.	1.9	53
74	Surface modification of goethite by phosphate for enhancement of Cu and Cd adsorption. Colloids and Surfaces A: Physicochemical and Engineering Aspects, 2007, 293, 13-19.	4.7	43
75	Effect of phosphate on the adsorption of Cu and Cd on natural hematite. Chemosphere, 2006, 63, 1235-1241.	8.2	55
76	Effects of Low Molecular Weight Organic Anions on the Release of Arsenite and Arsenate from a Contaminated Soil. Water, Air, and Soil Pollution, 2005, 167, 111-122.	2.4	27